ELSEVIER

Journal of Crystal Growth 240 (2002) 467–472

JOURNAL OF CRYSTAL GROWTH

www.elsevier.com/locate/jcrysgro

High-quality ZnO thin films prepared by two-step thermal oxidation of the metallic Zn

S.J. Chen[a], Y.C. Liu[a,b,*], J.G. Ma, D.X. Zhao[b], Z.Z. Zhi[a], Y.M. Lu[b], J.Y. Zhang[b], D.Z. Shen[b], X.W. Fan[b]

[a] *Institute of Theoretical Physics, Northeast Normal University, Changchun 130024, People's Republic of China*
[b] *Key Laboratory of Excited State Process, Chinese Academy of Sciences, 1-Yan An Road Changchun 130021, People's Republic of China*

Received 16 September 2001; accepted 11 February 2002
Communicated by R. James

Abstract

In this paper, we report the preparation of nanocrystalline ZnO thin films on Si (1 0 0) substrates using a simple method, in which a resistive thermal evaporation of Zn and a two-step annealing process were employed. The aim of the first annealing step in an oxygen ambient at 300°C for 2 h is to form ZnO layers on the surface of the Zn films to prevent the diffusion of the metallic Zn from the films during the high-temperature annealing process. To obtain high-quality ZnO films, a high-temperature annealing step was performed at temperature in the range of 600–900°C. The effects of the annealing temperature on the photoluminescence (PL) and orientation of ZnO nanocrystalline thin films were studied. A very strong near-band-edge emission around 375 nm with a full-width at half-maximum of 105 meV and a relatively weak emission around 510 nm related to deep-level defects were observed, which indicated that high-quality ZnO films have been obtained.

PACS: 68.60.Dv; 78.55.Et; 81.15.Fg; 81.65.Mq

Keywords: A1. Crystal structure; A1. Photoluminescence; A1. X-ray diffraction; A3. Physical vapor deposition processes; B1. Zinc compounds; B2. Semiconducting II–VI materials

1. Introduction

In recent years, wide band-gap semiconductor materials have attracted a great deal of attention for their use in blue light-emitting and short-wavelength laser diodes. ZnO, a well-known wide band-gap semiconductor, is gaining importance for the possible application as a semiconductor laser, because of its ultraviolet emission at room temperature (RT). It has a wide band gap of 3.3 eV at room temperature and a high exciton binding energy of 60 meV, which allow efficient UV emission from the exciton and make it suitable for UV laser-emitting devices. Moreover, ZnO is thermally and chemically stable in air. Hence, many different techniques, such as sputtering [1],

*Corresponding author. Fine Mechanics and Physics Key Laboratory of Excited State Process, Chinese Academy of Sciences, 1-Yan An Road, Changchun 130021, People's Republic of China. Tel.: +86-0431-5937596; fax: +86-0431-5955378.

E-mail address: ycliu@nenu.edu.cn (Y.C. Liu).

0022-0248/02/$ - see front matter
PII: S0022-0248(02)00925-9

reactive thermal evaporation [2], spray pyrolysis [3], pulsed laser deposition [4], metal organic chemical vapor deposition (MOCVD) [5], and molecular beam epitaxy (MBE) [6] have been used to prepare ZnO thin films. In most polycrystalline thin films, defect-related deep-level emissions dominate the PL spectra, which precludes various applications such as UV luminescent devices and unconventional polycrystalline lasers. Thus, obtaining pure crystalline material is a prerequisite for polycrystalline UV devices as well as for device efficiency and degradation prevention. Recently, Kim et al. reported that high-quality and high-purity ZnO films have been prepared by oxidation of metallic Zn [7].

In this paper, we report a simple method for preparing high-quality nanocrystalline ZnO thin films by using a resistive thermal evaporation technique followed by a two-step annealing process. The advantage of this process is that we can obtain more pure ZnO crystallites, because a pure Zn source can be used and no impurities are introduced during the process. Moreover, by taking into account that the melting point of metallic Zn is 419.5°C, the annealing process was divided into two steps. Firstly, all the films were oxidized to form ZnO layers on the surface of the metallic Zn films. The Zn oxidation was performed in an oxygen ambient at 300°C for 2 h to avoid Zn diffusion at high temperature. The Zn films were subsequently annealed in an oxygen ambient at 600°C, 700°C, 800°C and 900°C, respectively. In the room temperature PL spectra, strong and sharp near-band-edge emissions at 375 nm with very weak deep-level emission were obtained.

2. Experiments

The Zn metal films were deposited on Si (1 0 0) substrates at 200°C by resistive thermal evaporation of Zn. The substrates were pre-cleaned by normal method before deposition. The pressure of the growth chamber was on the order of 10^{-4} Pa. The thicknesses of the deposited Zn films were about 600 nm. After deposition, the films were oxidized in a thermal oxidation furnace. To prevent the evaporation of the metallic Zn from the films during the annealing process, we treated the films with a two-step annealing: all films were first oxidized in an oxygen ambient at 300°C for 2 h, then annealed in an oxygen ambient at 600°C, 700°C, 800°C and 900°C, respectively. To characterize the crystal structure of these films, X-ray diffraction (XRD) were measured using a D/max-rA X-ray diffraction spectrometer (Rigaku) with a CuK_α line of 1.54 Å and atomic force microscopy (AFM) studies. For the optical characterization, photoluminescence (PL) spectra were measured in the wavelength range of 350–625 nm. To obtain the binding energy of the free exciton, the dependence of the PL spectra of the samples on temperature was measured from 77 to 282 K. The 325 nm line of a He–Cd laser with a power of 50 mW was used as the excitation light.

3. Results and discussion

Fig. 1 shows the $\theta-2\theta$ XRD patterns of the as-deposited thin films and these films treated by a two-step annealing process. The Zn films are polycrystalline with a hexagonal close packed crystal lattice ($a = 2.665$, $c = 4.947$ Å). After the Zn thin film was oxidized at 300°C in O_2 ambient for 2 h, it underwent a partial transformation from Zn to ZnO. These films were next annealed in O_2 ambient for 1 h at 600°C, 700°C, 800°C and 900°C, respectively. The XRD patterns of the ZnO films indicated that they possessed a polycrystalline hexagonal wurtzite structure ($a = 3.250$, $c = 5.207$ Å) without a preferred orientation. Three main peaks appeared at $2\theta = 31.77°$, 34.62°, and 36.75°, which correspond to (1 0 0), (0 0 2), and (1 0 1) directions of the hexagonal ZnO structure, respectively. We observed that once the sample became fully oxidized, the c-axis orientation remained unchanged regardless of the oxidation temperature. As the annealing temperature increased, the (0 0 2) peak became prominent in comparison to other peaks. Moreover, all the peaks became sharper with increase of the annealing temperature due to increased particle size and improved crystal quality.

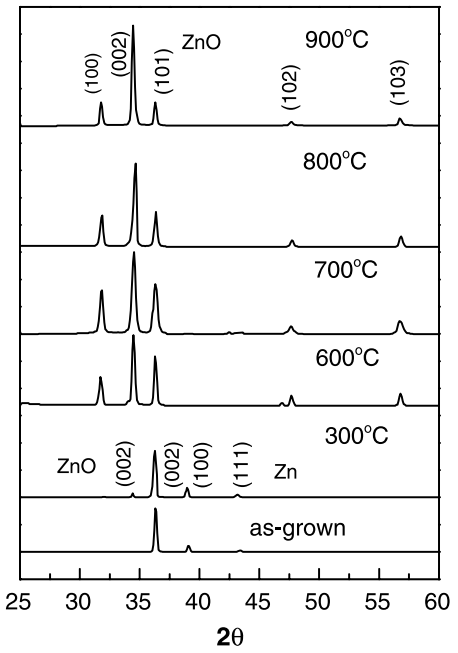

Fig. 1. XRD spectra of the as-grown Zn and the annealed ZnO thin films with different annealing temperatures.

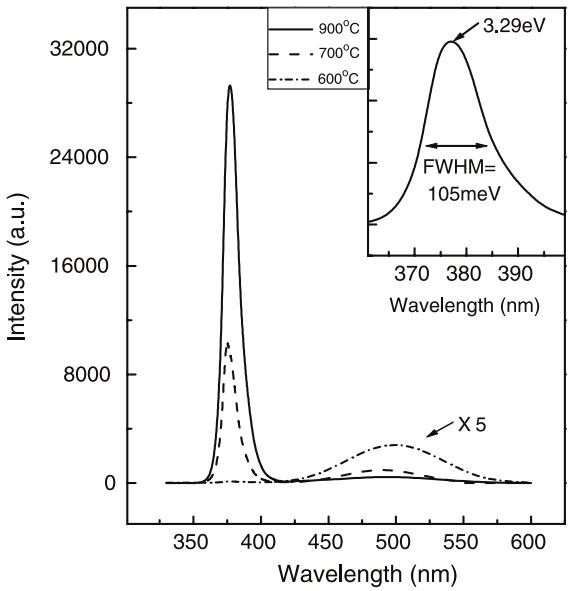

Fig. 2. Room temperature PL spectra of polycrystalline ZnO thin films annealed at different temperatures. The inset shows the peak position and FWHM of the sample annealed at 900°C.

Using Scherer formula [8]

$$d = \frac{0.9\lambda}{B\cos\theta}, \quad (1)$$

the mean grain sizes (d) of the films were evaluated. Here λ, θ, and B are the X-ray wavelength (1.54 Å), Bragg diffraction angle and line-width at half-maximum of (0 0 2) peak around 34.62°, respectively. The mean grain sizes of our samples are 22, 26.7, 34, 37 nm for the samples annealed at 600°C, 700°C, 800°C, and 900°C, respectively, which indicates that the particle size increases with increasing annealing temperature, as expected, resulting in the sharpened and enhanced diffraction peaks. The film roughness determined by AFM was in the range of 20–40 nm range, consistent with the XRD results.

Fig. 2 shows the room temperature PL spectra of the ZnO thin films annealed at different temperatures. An intense PL emission peak at 375 nm is observed. As the annealing temperature increases, the UV peak shifts to shorter wavelengths and becomes sharper with the increase of peak intensity. The full-width at half-maximum (FWHM) of PL peak at 375 nm is 105 meV for the sample annealed at 900°C as shown in the inset in Fig. 2. Moreover, the PL peak at around 510 nm related to deep-level emission is very weak. As the annealing temperature increases, this peak intensity decreases remarkably, and becomes almost negligible for the sample annealed at 900°C.

Fig. 3 shows the dependence of the PL spectra of the sample annealed at 700°C on temperature from 77 to 282 K. As the temperature increases, the UV peak shifts to longer wavelengths and its intensity decreases. In terms of the integrated PL intensity versus temperature, the quenching of the emission intensity with temperature was measured (see Fig. 4). To extract the binding energy, we fit the intensity PL data to the equation [9,10]

$$I(T) = I_0[1 + C\exp(-E/kT)]^{-1}, \quad (2)$$

where E is the binding energy of the exciton, and C contains ratios of optical-collection efficiencies and effective degeneracies of unbound and bound states. A fit to the data yields $E \approx 63$ meV for the sample annealed at 700°C. With the same method we have obtained the binding energies of free

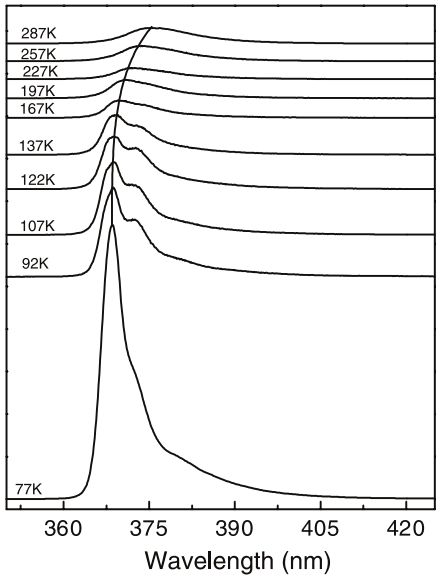

Fig. 3. PL spectra of the sample annealed at 700°C measured at varied temperatures.

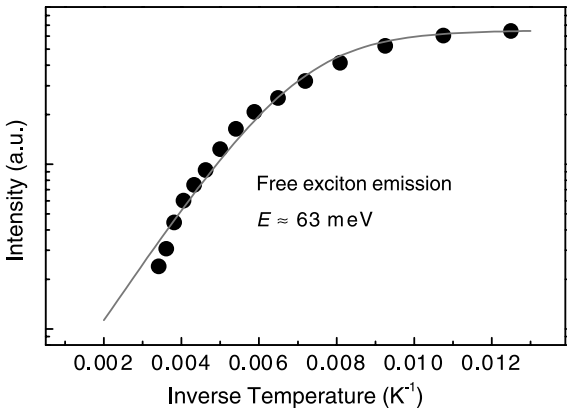

Fig. 4. The PL integrated intensity is plotted versus inverse temperature. Based on these data, the binding energy is estimated to be 63 meV.

excitons for other samples, the results are shown in Table 1.

It is well known that ZnO usually displays three major PL peaks: a UV band edge or near-band-edge emission peak around 380 nm, a green emission around 510 nm, and a red emission around 650 nm. It is generally accepted that the green and red emissions are associated with oxygen vacancies and interstitial oxygen in the

Table 1
Grain size and binding energy versus annealing temperature

Annealing temperature (°C)	600	700	800	900
Grain size (nm)	22	26.7	34	37
Binding energy (meV)	65	63	58.2	53.5

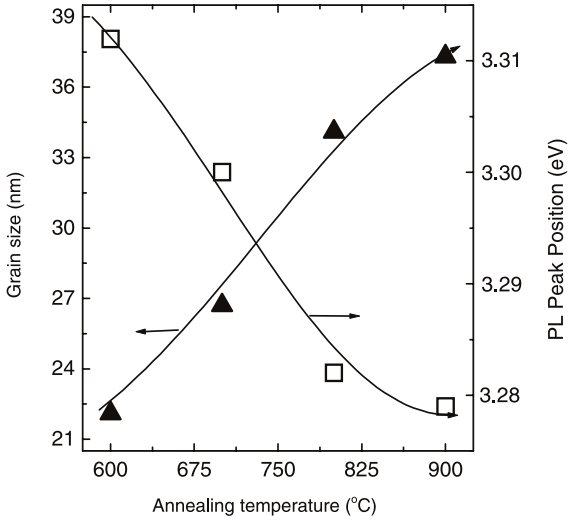

Fig. 5. Grain size and PL peak position versus annealing temperature.

ZnO lattice. One way to evaluate the concentration of structural defects in ZnO is to compare the PL intensity ratio of the UV near-edge emission to the deep-level green emissions. The reported PL spectra of powder or polycrystalline thin films have shown much stronger deep-level emission than UV emission, resulting in a relative PL intensity ratio of zero at room temperature. Our nanocrystalline ZnO films displayed a very strong UV emission around 374–380 nm (3.316–3.260 eV) and a very weak green emission. As the annealing temperature increases, the PL peak position moves to longer wavelengths, from 374 to 380 nm, and the grain size increases from 22 to 37 nm, as shown in Fig. 5. The shift of the exciton peak with particle size is probably due to a quantum-confinement-induced energy gap enhancement. An expression [11] for the energy gap, including

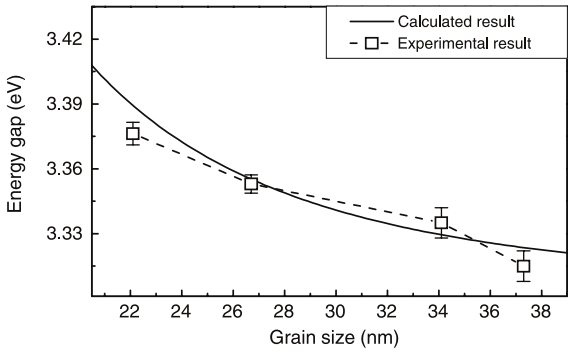

Fig. 6. Energy gap versus grain size, in which the solid line corresponds to the calculated result, and the dash line with open square symbols correspond to experimental results.

the quantum confinement effect, is

$$E_g \approx E_{g0} + \frac{h^2\pi^2\mu}{2d^2} - \frac{1.8e^2}{\varepsilon d}, \quad (3)$$

where E_{g0} is the energy gap for bulk materials, d is the particle size, $1/\mu = 1/m_e + 1/m_h$ (m_e and m_h being the electron and hole effective masses, respectively), and ε is the dielectric constant. For ZnO, the effective masses of electrons and holes are $0.38m_0$ and $1.80m_0$ [12], respectively, and the dielectric constant is 8.75. Thus, we obtain

$$E_g(\text{eV}) \approx E_{g0} + 75.885d^{-2}\ (\text{nm})^2 - 1.902d^{-1}\ (\text{nm}). \quad (4)$$

Fig. 6 shows the energy gap versus grain size of ZnO, in which the solid line corresponds to the calculated result and the dash line with open square symbols correspond to the experimental results. Our experimental result is in a good agreement with the calculated result, in which the energy gap is the sum of the peak energy and binding energy. In addition, the very weak deep-level emission and small UV FWHM in our films indicate that the concentrations of the defects responsible for the deep-level emissions are relatively low.

4. Conclusions

In summary, nanocrystalline ZnO thin films with intense UV emission were prepared by two-step annealing of the metallic Zn film in an O_2 ambient. After the films were annealed following first step at 300°C, the metallic Zn on the surface of Zn films was partially oxidized into ZnO, so metallic Zn could not diffuse from Zn films during the second-step annealing process at higher temperature. After annealing at 600°C, 700°C, 800°C and 900°C, respectively, all of the Zn was transformed to ZnO. As the annealing temperature was increased, the grain size increased and the PL peak position shifted to longer wavelengths. The PL spectrum showed a strong UV emission peak around 375 nm at room temperature, corresponding to the ZnO free excition emission. The very weak deep-level emission and small FWHM in our films indicate that the concentrations of the defects responsible for the deep-level emissions are relatively low.

Acknowledgements

This work was supported by the Program of CAS Hundred Talents, the National Natural Science Foundation of China, the Innovation Foundation of CIOFP, Excellent Young Teacher Foundation of Ministry of Education of China, and Jilin Distinguished Young Scholar Program.

References

[1] H. Nanto, T. Minami, S. Takata, Phys. Stat. Sol. A 65 (1981) K131.
[2] H. Morgan, D.E. Brodie, Can. J. Phys. 60 (1982) 1387.
[3] J. Aronovich, A. Ortiz, R.H. Bube, J. Vac. Sci. Technol. 16 (1979) 994.
[4] R.D. Vispute, V. Talyansky, S. Choopun, R.P. Sharma, T. Venkatesan, M.He.X. Tang, J.B. Halpern, M.G. Spencer, Y.X. Li, L.G. Salamanca-Riba, A.A. Iiiados, K.A. Jones, Appl. Phys. Lett. 73 (1998) 348.
[5] S. Bethke, H. Pan, B.W. Wesseis, Appl. Phys. Lett. 52 (1988) 138.
[6] Y. Chen, D.M. Bagnall, H.J. Koh, K.T. Park, K. Hiraga, Z. Zhu, T. Yao, J. Appl. Phys. 84 (1998) 3912.
[7] J.C. Kim, H. Rho, L.M. Smith, H.E. Jackson, Appl. Phys. Lett. 75 (1999) 214.
[8] B.D. Cullity, Elements of X-ray Diffractions, Addison-Wesley, Reading, MA, 1978, p. 102.

[9] J.C. Kim, H. Rho, L.M. Smith, H.E. Jackson, S. Lee, M. Dobrowolska, J.K. Furdyna, Appl. Phys. Lett. 76 (1999) 214.
[10] R.E. Dietz, J.J. Hopfield, D.G. Thomas, J. Appl. Phys. 32 (1961) 2282.
[11] S. Cho, J. Ma, Y. Kim, Y. Sun, G.K.L. Womg, Appl. Phys. Lett. 75 (1999) 2761.
[12] L.E. Brus, J. Chem. Phys. 80 (1984) 4403.